SEISMOELECTRIC LABORATORY MEASUREMENTS IN A BOREHOLE

Zhenya Zhu and M. Nafi Toksöz

Earth Resources Laboratory
Department of Earth, Atmospheric, and Planetary Sciences
Massachusetts Institute of Technology
Cambridge, MA 02139

ABSTRACT

The seismoelectric logging method is based on measuring the electric field generated by seismic waves in a fluid-filled borehole. Two kinds of electromagnetic (EM) fields can be generated within the formation and at the interface of formations. One is a stationary or local EM wave and the other is a radiating EM wave. In this paper, we make various fractured borehole models with artificial materials or natural rocks and measure the electric field generated by a seismic source in a water-filled borehole. The experimental results show that the Stoneley wave generates both a stationary EM wave at the borehole wall and a radiating EM wave on the fracture, which propagates with light speed in the borehole. When the aperture of the fracture increases, the amplitude of the seismoelectric wave decreases due to the low ion concentration in the fracture. In a layered borehole model, a thin, permeable glued-sand zone is sandwiched between two nonpermeable or low-permeable layers, and the Stoneley wave generates two kinds of seismoelectric signals at the permeable zone. Compared with the acoustic waveforms in the same borehole, the seismoelectric waveforms are more effective in determining and characterizing a fracture or a fractured zone filled with a permeable layer.

INTRODUCTION

At the interface between fluid and solid, adsorption of electric charge to the surface of the solid creates an excess of mobile ions of opposite charge to that of the fluid (Bockris and Reddy, 1970). Thus, a double layer is formed on the solid surface. When a seismic wave propagates in a two-phase medium of solid and fluid, the mechanic waves generates a movement of ions in the fluid. The movement of the charges induces an electromagnetic (EM) field. This phenomenon, that a seismic wave induces an electromagnetic wave in a two-phase medium, is referred to as seismoelectric conversion. On the other hand, when an outside electric field induces vibration of the charges in the fluid, the interaction between fluid and solid generates a seismic wave. This process is referred to as electroseismic conversion.

Theoretical studies (Pride and Haartsen, 1996; Haartsen, 1995) confirm the mechanism of these conversions. Inside the homogeneous, porous medium, the seismic wave induces a stationary seismoelectric field which exists only in the area disturbed by the seismic wave. At the interface of formations with different properties, such as porosity, permeability, or lithology, the seismic wave induces a radiating seismoelectric wave which propagates with light speed and can be received anywhere.

Early laboratory experiments focused on the measurements of the streaming potentials generated by low frequency (under 1000 Hz) vibration or steady fluid flow in a fluid-saturated porous medium (Cerda and Kiry, 1989). Recent laboratory experiments observed the seismoelectric conversion at high frequency (kHz) range (Zhu and Toksöz, 1996).

Recent surface experiments in the field (Thompson and Gist, 1993; Butler *et al.*, 1996; Mikhailov *et al.*, 1997a) confirm that seismoelectric signals from various interfaces in the subformation can be detected. Due to the exponential decay of the electric field in a conductive medium, this method has a limited penetration depth in field measurements. It is difficult to apply this method to the exploration of petroleum geology. Field experiments (Mikhailov *et al.,* 1997b) have been conducted in a borehole, but also show depth limitation because the source was at the surface.

To overcome the above limitation and to apply this method to petroleum geophysics, we have focused our studies on borehole measurements of seismoelectric conversion and developed a new method called "seismoelectric logging in a borehole." The experimental results of our studies show that the seismoelectric signals can be generated by the acoustic source in a borehole and measured by an electrode in the same borehole (Zhu and Toksöz, 1997). These measurements can be applied to both shallow and deep boreholes and obtain detailed information about fluid flow in the formation.

In this paper, we conduct seismoelectric measurements in fractured borehole models. Both the acoustic source and the electrode are in the same borehole. When the Stoneley wave propagates past a fracture, it generates a flow of ion-carrying fluid in the fracture, thus creating a radiating electromagnetic wave that propagates with light speed in the borehole and surrounding formations. By recording and comparing the electric signals and acoustic waves generated by the same acoustic source, we investigate which measurements more easily identify a fracture or fractured zone.

BOREHOLE MODELS AND MEASUREMENTS

To simulate a fracture intersecting a borehole, we make borehole models of two separate cylinder blocks with boreholes in their centers (Figure 1). The materials of the blocks are artificial material (Lucite) or natural rock (slate). The diameter of the borehole is

1.27 cm. Three models are composed of two Lucites, two slates, and one Lucite and one slate, respectively. Between the two blocks there is a gap, saturated with water (Figure 1a). Figure 1b shows a layered borehole model where a thin epoxy-glued sand layer is sandwiched between two slate or Lucite blocks.

During the measurements, a PZT-tube transducer, 0.9 cm in diameter, is placed at the lower section of the borehole and excited by an electric square pulse of 10 μs in width and 750 V in amplitude. The electrode is a point receiver, 0.5 mm in diameter and 1.0 mm in length, made of a shielding cable wire. After going through a pre-amplifier with 60 dB gain and a filter, the received electric signals are displayed and recorded on a digital oscilloscope (Zhu and Toksöz, 1996). The whole model with the source transducer and the electrode are soaked in water whose conductivity is about 0.18 mS.

We fix the source transducer at the lower section of the borehole, move the electrode along the borehole and across the fracture, and record the received electric signals at each step. All recorded electric waveforms are time delayed to avoid the huge electric influence by the high-voltage source pulse.

To compare the electric signals with the acoustic field in a borehole, a hydrophone (B&K 8103) replaces the electrode and measures the acoustic waveforms under the same conditions. The amplitude of the acoustic waveforms are normalized by the maximum in each plot.

RESULTS IN FRACTURED BOREHOLE MODELS

We perform experiments in three borehole models composed of two blocks with a water-filled gap (Figure 1a). The materials of the two blocks are Lucite-Lucite, slate-slate, and slate-Lucite, respectively. The aperture of the gap is 0.2 mm.

Figure 2 shows the electric signals (Figure 2a) and the acoustic waves (Figure 2b) in the Lucite-Lucite borehole model. From the acoustic waveforms (Figure 2b), we know that there is a fracture around trace 7. At the fracture, the Stoneley wave generates a P-wave propagating across the fracture and into the upper section. The Stoneley wave splits into two waves propagating with P-wave and Stoneley wave velocities, respectively. In Figure 2a the amplitudes of the electric waveforms are normalized by the clip voltage of 2μV. We see some electric components propagating with Stonely wave velocity. They are stationary electromagnetic waves generated by the Stoneley wave. There is another electric component which starts from the fracture (trace 7) and propagates with high speed. It arrives at the same time on each trace. Because the Stoneley wave forces the ion-carrying water in the fracture to vibrate horizontally, the flow of free charge in the fluid induces a radiating electromagnetic wave which can be received at any place in the borehole.

In a nonpermeable Lucite model, a double layer forms on the borehole wall and on the surfaces of the fracture. When a surface wave (Stoneley wave) propagates along a borehole, the wave excites the borehole wall and the ions attached to the wall to vibrate. Because of the consistency of the borehole along its axis and the direction of wave propagation, the Stoneley wave generates a stationary electromagnetic wave at the wall. Only at the fracture does the Stoneley wave generate the radiating electromagnetic wave.

To investigate the effect of a fracture aperture on the seismoelectric conversion, we change the aperture between the two Lucite blocks and measure the electric signals. Figure 3 shows the relationship between the aperture of a fracture and the amplitude of the seismoelectric signal generated by the Stoneley wave in the borehole model. The larger the aperture, the smaller the amplitude of the electric signal. The number of free ions in the fluid depends on the surface area. When the aperture increases, the surface area and the number of free ions do not increase. Because the concentration of ions in the fracture decreases, the strength of the streaming electric current generated by the same Stoneley wave decreases. These results confirm that the seismoelectric signals at a fluid-saturated fracture are related to its aperture and the electrochemical properties of the fractured formation.

The same measurements are conducted with slate-Lucite and slate-slate borehole models. Figure 4 shows the seismoelectric signals (Figure 4a) and the acoustic waves (Figure 4b) in the slate-Lucite model. The acoustic source is fixed in the slate section. Slate is a very hard rock, and its P-wave velocity is 6,950 m/s. Therefore, the acoustic source generates a stronger Stoneley wave in the slate section than in the previous Lucite-Lucite model. At trace 7 in Figure 4b, the Stoneley wave splits into both a P-wave and a Stoneley wave in the Lucite section. This confirms that there are two materials with a fracture between them. From the slopes of the seismoelectric signals in Figure 4a, we know that the Stoneley wave generates a stationary EM signal at both the slate and Lucite sections, and it generates a radiating EM signal at the fracture. The signal is received in the Lucite section. Compared with the radiating signal in the Lucite-Lucite model (Figure 2a), the radiating EM signal is stronger in the slate-Lucite model (Figure 4a). Therefore, the seismoelectric conversion is related to the electrochemical properties of the fracture formation.

Figure 5 shows the electric signals (Figure 5a) and the acoustic waves (Figure 5b) recorded in the slate-slate borehole model. The Stoneley wave velocity is the same in both slate sections. We can see that the amplitude of the Stoneley wave becomes smaller at the fracture (traces 6 and 7 in Figure 5b). The P-wave is very weak in this hard rock model. In Figure 5a, we observe the seismoelectric signals generated by the Stoneley wave. We also record the radiating EM signals, which are generated at the fracture. These signals have the same arrival time on each trace with the Stoneley wave arriving at the measurement points later. In this model, the amplitude of the signals is smaller than in previous borehole models because it depends not only on the fracture aperture, but also on the electrochemical properties of the surrounding rock.

Our experiment results show that a radiating EM wave is an indicator for a fracture or fractured zone. When the borehole is surrounded by the same formation, the Stoneley wave generates a seismoelectric signal that propagates with the same velocity. If the Stoneley wave generates an electric signal that propagates with electromagnetic speed, it means there is a fracture or fractured zone in the borehole.

RESULTS IN SANDWICHED BOREHOLE MODELS

In order to simulate a borehole that is intersected by a fracture filled with a thin permeable layer, we perform experiments with a borehole model where a thin, epoxy-glued sand layer is sandwiched between the slate or Lucite blocks (Figure 1b). The same procedures are conducted to record the seismoelectric signals and the acoustic waves in these models as were conducted in the experiments above.

Figure 6 shows the electric signals (Figure 6b) and the acoustic waves (Figure 6a) in the slate-sand-slate sandwiched borehole model. The thickness of the epoxy-glued sand layer is 1.0 cm. The amplitudes of the electric waveforms in Figure 6b are normalized by the clip voltage of 12μV. Figure 6c shows the amplitude of the electric signals normalized by the amplitude of the Stoneley waves at each trace.

From Figure 6a, we see that the amplitude of the Stoneley wave is large before the electrode enters the fracture (traces 1–5). When the acoustic wave enters the sand layer, the amplitude decreases due to its high attenuation, but the Stoneley wave velocity hardly changes. We can also see that the Stoneley wave generates a stationary seismoelectric wave that propagates with the same velocity (Figure 6b). The amplitude of the electric signals is larger at the sand layer due to its high porosity and permeability. Figure 6c shows the amplitude of this electric field normalized by the amplitude of the Stoneley wave at each trace. The amplitude peak at trace 7 indicates the sand formation with high porosity and high permeability. In Figure 6b we also see the radiating electromagnetic wave generated at the sandwiched sand layer due to the contact of the formations and possible gaps between the layers. This radiating electromagnetic wave propagates in the borehole with very high velocity. In this case, the center frequency of the electric signals is about 30 kHz, and it is higher at the slate section and lower at the glued-sand section. Thus, the frequency response is related to the lithology of the formation. The curve in Figure 6c is not clear enough to determine the thickness of the sand layer because the center frequency varies and the stationary and radiating signals interact.

We perform similar experiments with a model where a thin, glued-sand layer, 1.0 cm in thickness, is sandwiched between two Lucite blocks. Figures 7a and 7b show the acoustic waves and the seismoelectric signals recorded in the Lucite-sand-Lucite borehole model. Figure 7c shows the amplitude of the electric signals normalized by the amplitude of the Stoneley wave at each trace. The normalized amplitude of the seismoelectric signals at the glued-sand layer is much larger than that in the Lucite sections due to its high porosity and permeability. From the waveform variation of the electric signals, we see there still is a radiating component in Figure 7c, but it is difficult to separate it from the main signals because the frequency of the signal is too low and the glued-sand layer is too thin.

The experimental results confirm that the normalized amplitude of the electric signals is a good indicator for a fracture filled with a porous medium.

CONCLUSIONS

In this paper, we measure seismoelectric signals generated by Stoneley waves in boreholes with water or a porous medium filled fractures. The experimental results show that a stationary electromagnetic wave is induced at the borehole walls and a radiating electromagnetic wave is induced at fractures. In the water-filled fracture, the amplitude of the seismoelectric signals is related to its fracture aperture. The larger the aperture, the smaller the amplitude of the seismoelectric signals. In porous medium filled fractures, the Stoneley wave generates a stationary electric wave which is larger than a stationary electric wave in the nonpermeable formation. The Stoneley wave also generates a radiating seismoelectric wave at the interface between the porous medium and nonporous formation. Comparison of seismoelectric signals with the acoustic waves shows that it is easer to identify a fracture with seismoelectric signals than acoustic waveforms. The seismoelectric logging is an effective new logging method to explore fractures and fractured zones in boreholes.

ACKNOWLEDGMENTS

We thank Dr. M. W. Haartsen, Mr. O. V. Mikhailov, Prof. Steven R. Pride, and Prof. T. R. Madden for their valuable suggestions and useful discussions.

This study was supported by the Borehole Acoustics and Logging/Reservoir Delineation Consortia at M.I.T. and by the Department of Energy grant #DE-FG02-93ER14322.

REFERENCES

Bockris, J. and A.K.N. Reddy, 1970, *Modern Electrochemistry,* Plenum Press.

Butler, K., R. Russell, A. Kepic, and M. Maxwell, 1996, Measurement of the seismoelectric response from a shallow boundary, *Geophysics, 61*, 1769–1778.

Cerda, C.M. and N.-C. Kiry, 1989, The use of sinusoidal streaming flow measurements to determine the electrokinetic properties of porous media, *Colloids and Surfaces, 35*, 7–15.

Haartsen, M.W., 1995, Coupled electromagnetic and acoustic wavefield modeling in poro-elastic media and its application in geophysical exploration, Ph.D. thesis, MIT.

Mikhailov, O.V., M.W. Haartsen, and M.N. Toksöz, 1997a, Electroseismic investigation of the shallow subsurface: Field measurements and numerical modeling, *Geophysics, 62*, 97–105.

Mikhailov, O.V., J.H. Queen, and M.N. Toksöz, 1997b, Using borehole electroseismic measurements to detect and characterize fractured (permeable) zones, *67th SEG Annual International Meeting Expanded Abstracts, SS4.8*, 1981–1983.

Pride, S.R. and M.W. Haartsen, 1996, Electroseismic wave properties, *J. Acoust. Soc. Am., 100*, 1301–1315.

Thompson, A.H. and G.A. Gist, 1993, Geophysical applications of electrokinetic conversion, *The Leading Edge, 12*, 1169–1173.

Zhu, Z. and M.N. Toksöz, 1996, Experimental studies of seismoelectric conversion in fluid-saturated porous medium, *SEG 66th Annual International Meeting Expanded Abstracts, RP1.6,* 1699–1702.

Zhu, Z. and M.N. Toksöz, 1997, Experimental studies of electrokinetic conversion in fluid-saturated borehole models, *67th SEG Annual International Meeting Expanded Abstracts, BH3.13*, 334–337.

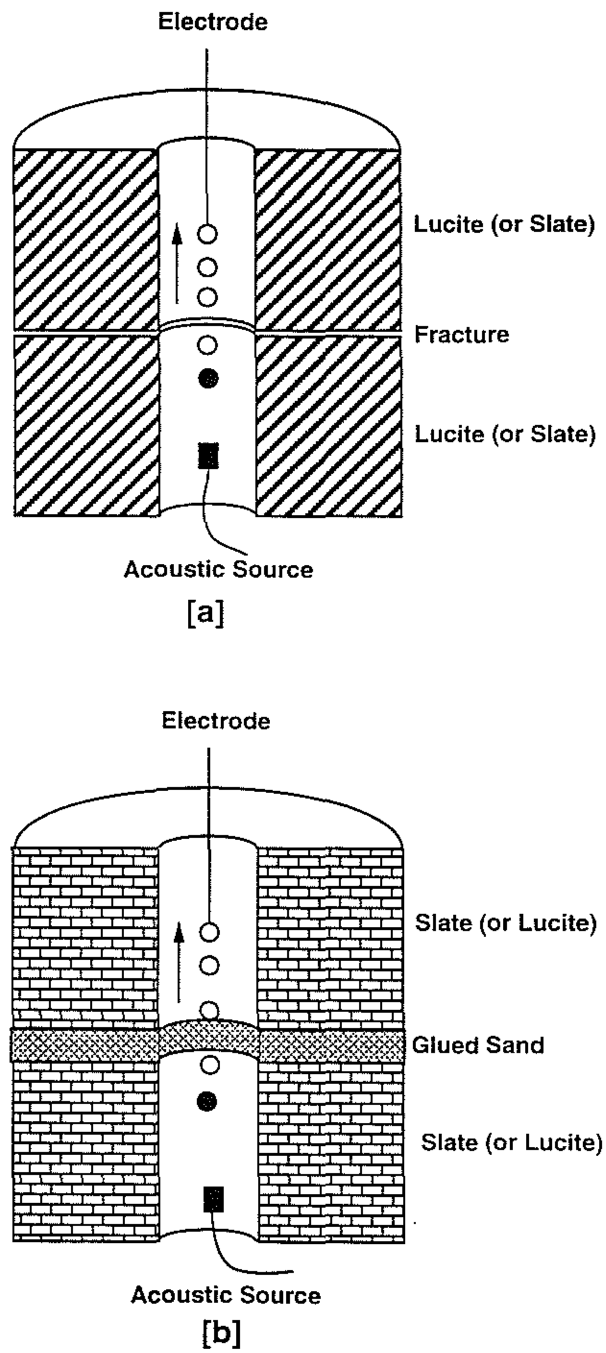

Figure 1: Diagram for measuring the seismoelectric field in the borehole model with a water-filled fracture (a) and a glued-sand layer (b). The aperture of the fracture is 0.2 mm. The thickness of the sand layer is 10 mm. The diameter of the borehole is 12.7 mm. An electric square pulse of 1000 V generates the acoustic source.

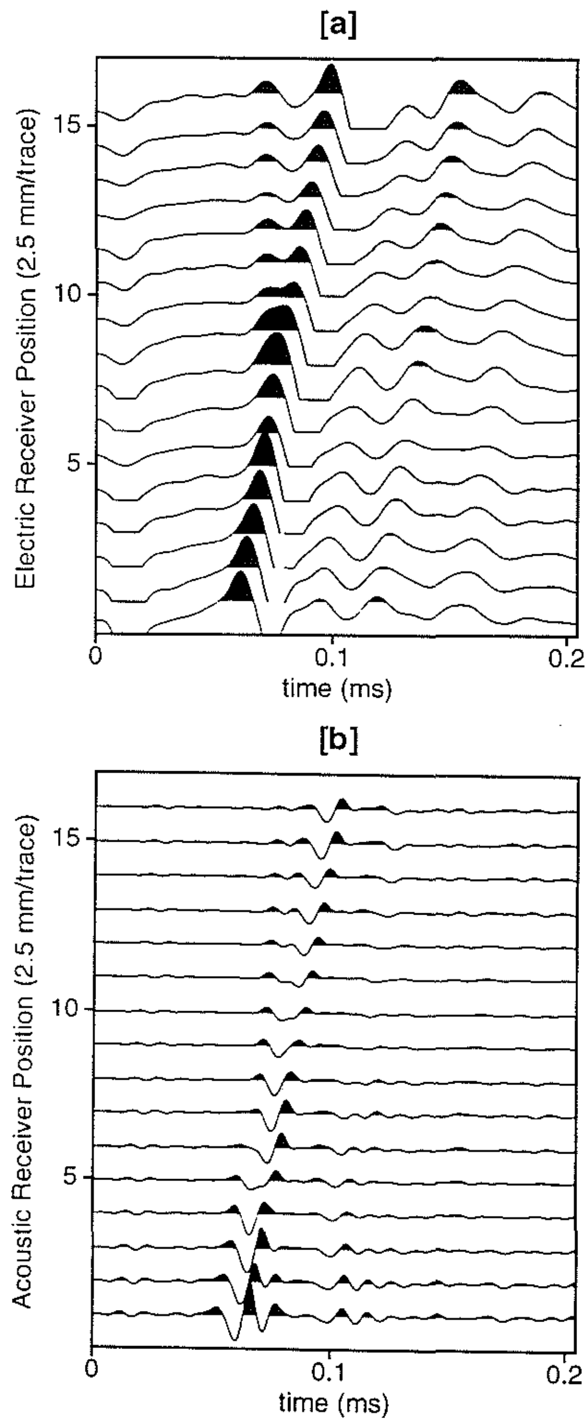

Figure 2: Seismoelectric signals (a) and acoustic waveforms (b) recorded in the Lucite-Lucite borehole model (Figure 1a). Trace 7 is at the fracture with an aperture of 0.2 mm. The amplitude of the seismoelectric signals (a) is normalized by $2\mu V$. The acoustic waves are normalized by the maximum amplitude of all waveforms.

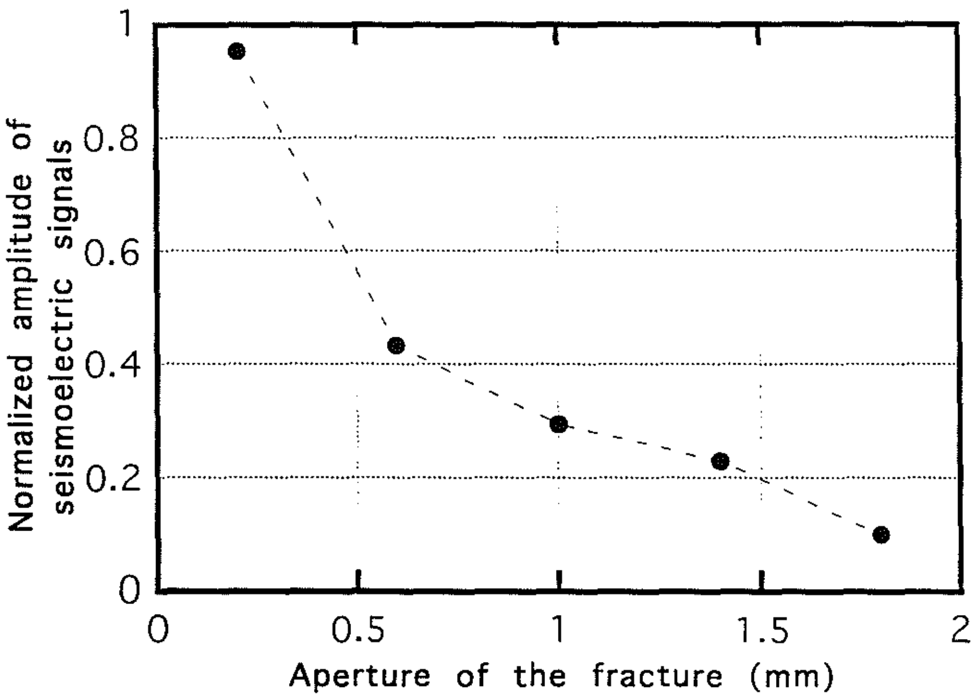

Figure 3: The relationship between the aperture of a fracture and the amplitude of the seismoelectric signal generated by the Stoneley wave in the Lucite-Lucite borehole model.

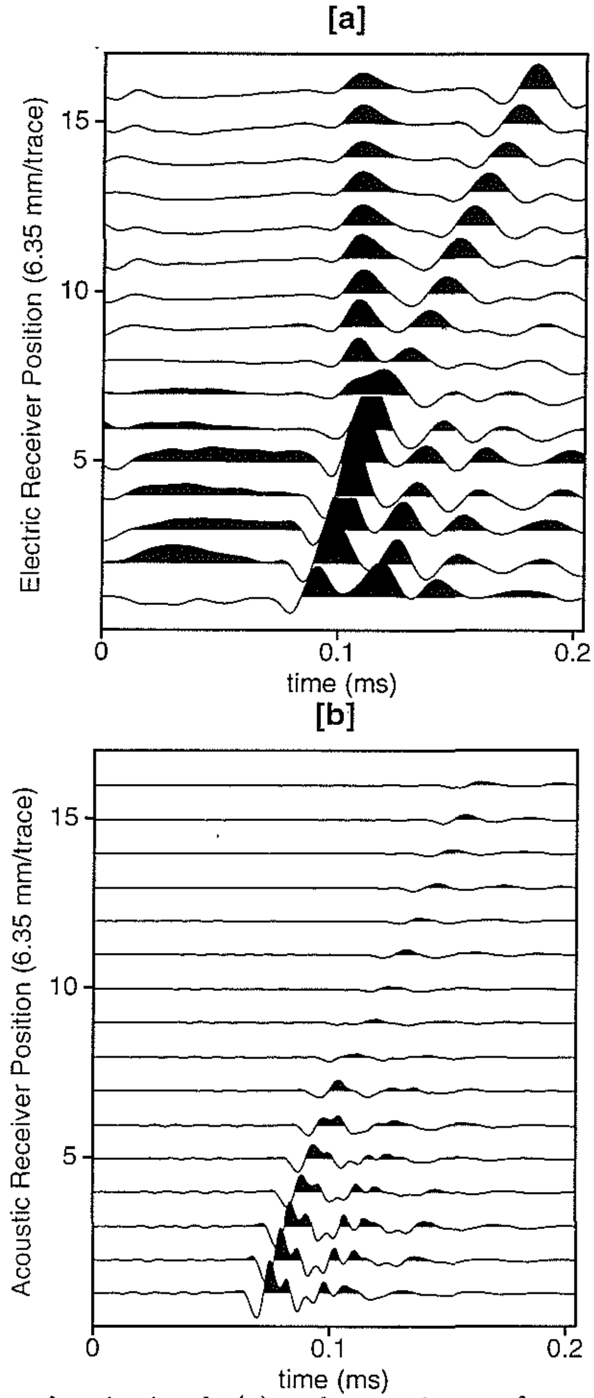

Figure 4: Seismoelectric signals (a) and acoustic waveforms (b) recorded in the slate-Lucite borehole model (Figure 1a). The acoustic source is located in the slate section. Trace 7 is at the fracture which has an aperture of 0.2 mm. The amplitude of the seismoelectric signals (a) is normalized by $12\mu V$. The acoustic waves are normalized by the maximum amplitude of all waveforms.

[a]

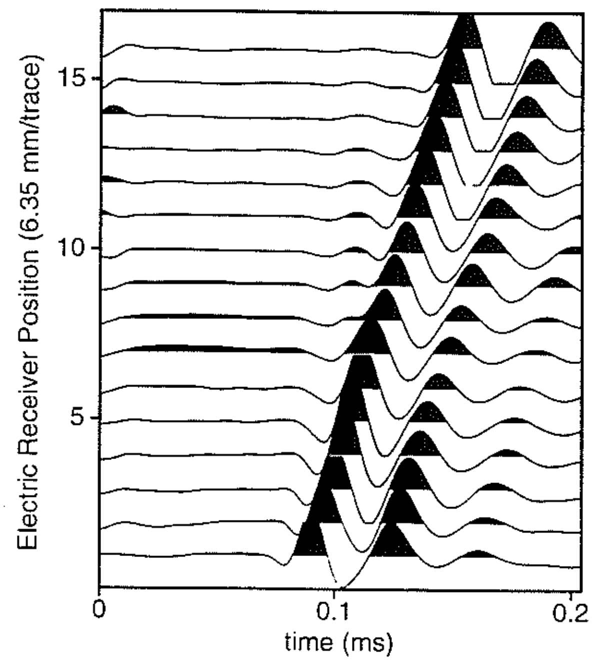

[b]

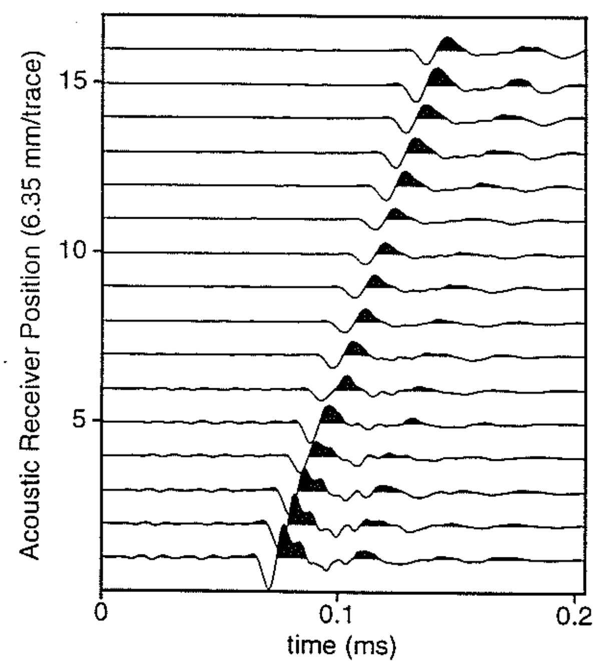

Figure 5: Seismoelectric signals (a) and acoustic waveforms (b) recorded in the slate-slate borehole model (Figure 1a). Trace 7 is at the fracture, which has an aperture of 0.2 mm. The amplitude of the seismoelectric signals (a) is normalized by $12\mu V$. The acoustic waves are normalized by the maximum amplitude of all waveforms.

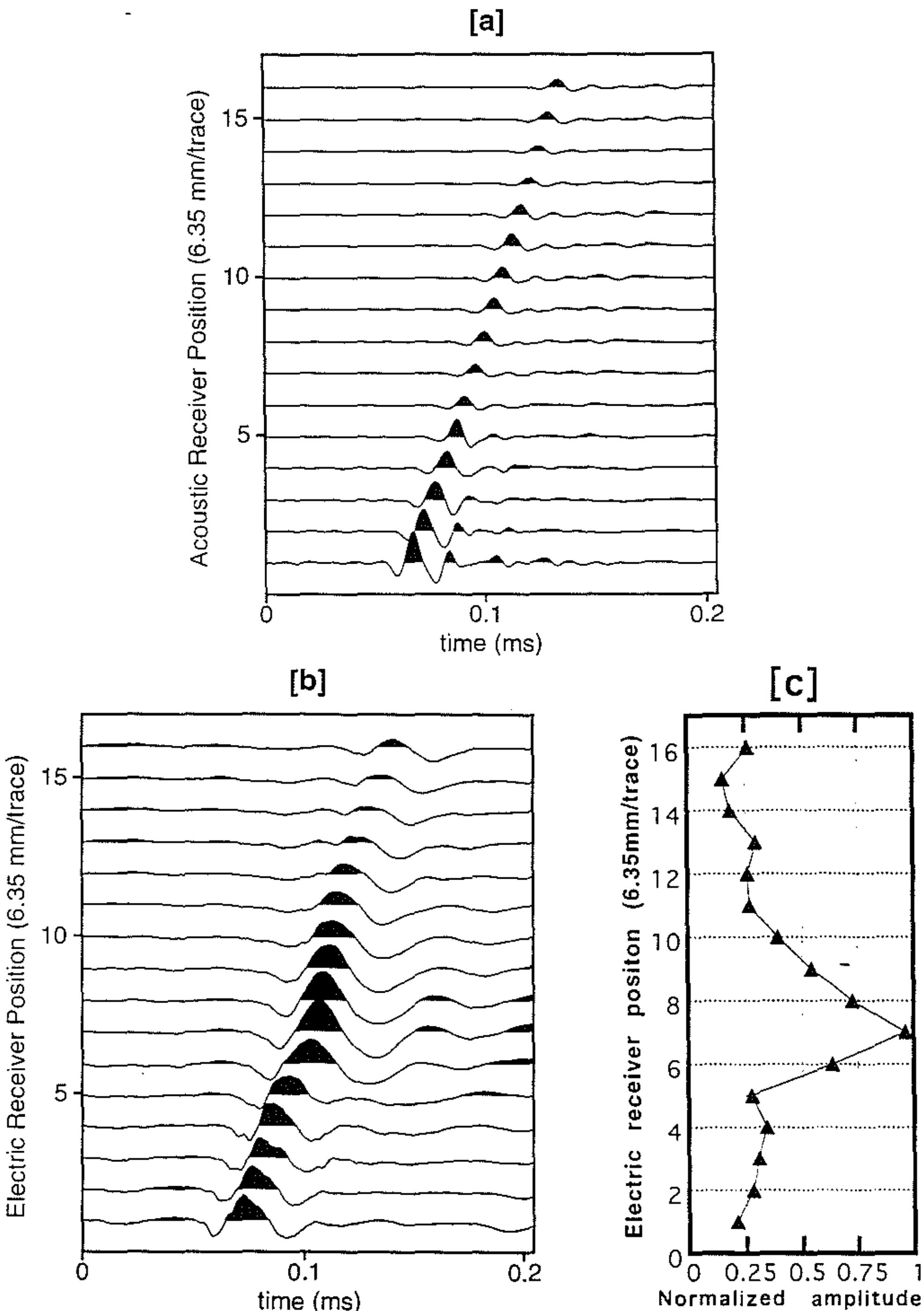

Figure 6: The acoustic waves (a) and electric signals (b) in the slate-sand-slate sandwiched borehole model (Figure 1b). The acoustic waves (a) are normalized by the maximum amplitude of all waveforms. The amplitude of the seismoelectric signals (b) is normalized by 12μV. Figure 6c shows the amplitude of the electric signals normalized by the amplitude of the Stoneley wave at each trace.

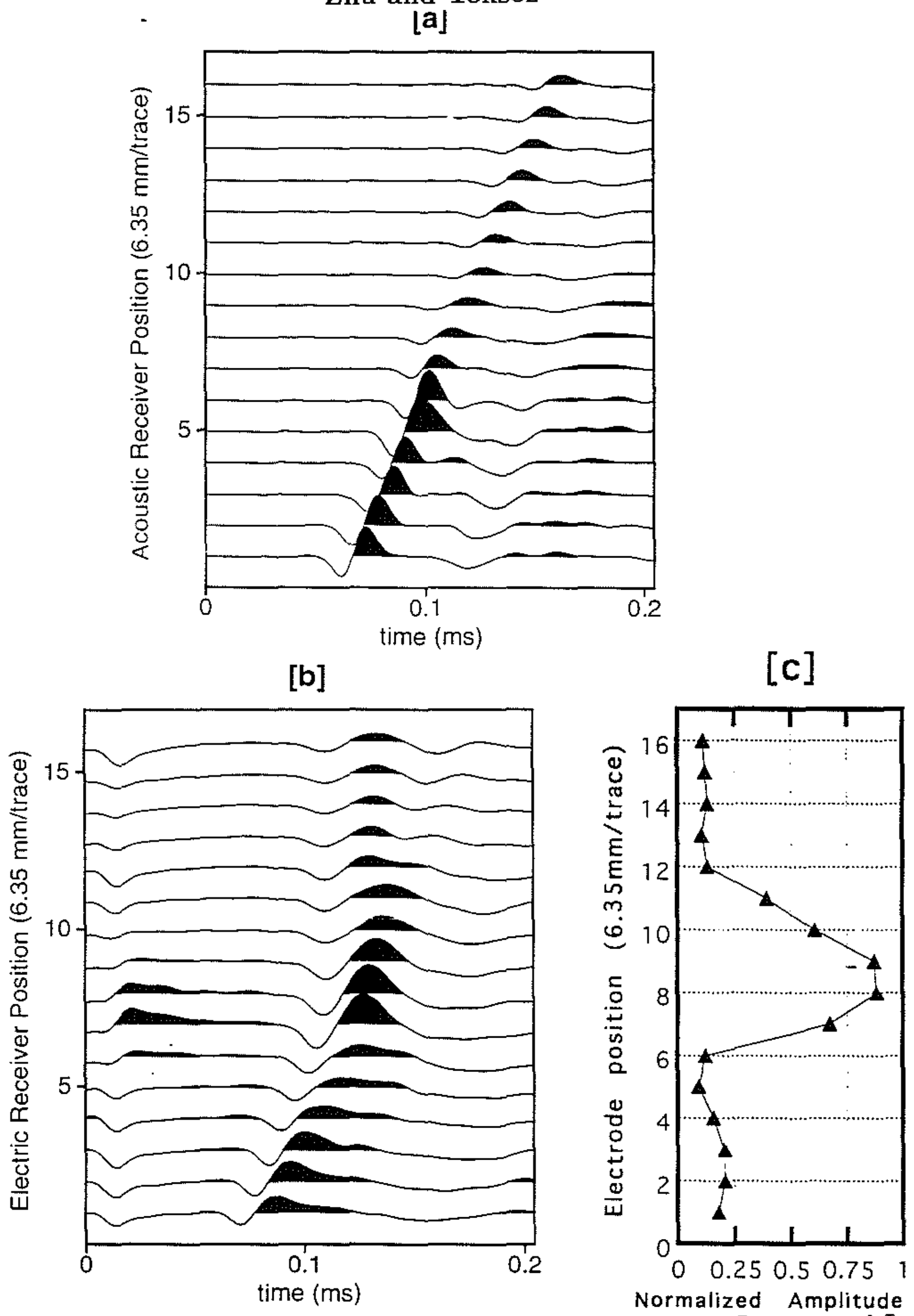

Figure 7: The acoustic waves (a) and electric signals (b) in the Lucite-sand-Lucite sandwiched borehole model (Figure 1b). The acoustic waves (a) are normalized by the maximum amplitude of all waveforms. The amplitude of the seismoelectric signals (b) is normalized by $12\mu V$. Figure 7c shows the amplitude of the electric signals normalized by the amplitude of the Stoneley wave at each trace.